

The following article is the final version submitted to IEEE after peer review; hosted by PTB; DOI: [10.1109/AMPS50177.2021.9586012](https://doi.org/10.1109/AMPS50177.2021.9586012). It is provided for personal use only.

Traceable calibration system for non-conventional current sensors with analogue or digital output

Y. Chen, E. Mohns, M. Seckelmann and S.de Rose

Acknowledgement: The presented work is used in the project 17IND06 (FutureGrid II) which have received funding from the EMPIR programme co-financed by the Participating States and from the European Union's Horizon 2020 research and innovation programme.

© 2018 IEEE. This is the author's version of an article that has been published by IEEE. Personal use of this material is permitted. Permission from IEEE must be obtained for all other uses, in any current or future media, including reprinting/republishing this material for advertising or promotional purposes, creating new collective works, for resale or redistribution to servers or lists, or reuse of any copyrighted component of this work in other works.

Full Citation of the original article published by IEEE:

Y. Chen, E. Mohns, M. Seckelmann and S. de Rose, "Traceable calibration system for non-conventional current sensors with analogue or digital output," *2021 IEEE 11th International Workshop on Applied Measurements for Power Systems (AMPS)*, 2021, pp. 1-6, doi: 10.1109/AMPS50177.2021.9586012.

Available at: <https://ieeexplore.ieee.org/document/9586012>

high current generation system (marked as red block), a set of analogue reference CTs (marked as green block) with associated precision resistors [8] and a precision 2-channel measuring system (marked as purple block) [9], [10]. The synchronization signals (marked as “Sync.” in blue) and the SV receiver box (shown as a grey block) are necessary when the output of the device under test (DUT) is a sampled value (SV) data stream.

The high current generation system consists of a programmable two-channel arbitrary waveform generator, a lowpass filter, a transconductance power amplifier and the high current generating transformers. Firstly, the arbitrary waveform generator, e.g., the Agilent 33500B Series with resolution of 16 Bit, generates different test waveforms, which reproduce PQ phenomena. The lowpass filter is to used limit the slew rate and the bandwidth of the generated signal with adjustable amplitudes. The generated signal is in turn amplified by the transconductance power amplifier (up to 270 V_{rms} / 70 A_{rms}, DC to 15 kHz) and by the high current generation transformers with several rated current ranges from 5 A to 1 kA rated. The laboratory generation capabilities are tested with frequencies ranging from 50 Hz to 5 kHz. Sinusoidal waveforms up to 2 kA, dual-tone or multi-tone waveforms up to 2 kA and amplitude modulated waveforms are generated. The limitation at frequencies above 500 Hz is caused by the internal stray inductance of the high current generation transformer.

The synchronization plays a significant role for the phase measurement processes of the SV-based devices and the digital signal processing between different devices within the substation. The synchronization signals can be obtained by two laboratory global positioning system (GPS) receivers: the “Meinberg GPS 162” and the “NI-PXI-6683”. The synchronization signals are regarded as the time references for the calibration systems and are transmitted as 10 MHz, pulse per second (PPS) and IEEE 1588-2008 (PTPv2) protocol. Besides, the White Rabbit LENs [11], which are completely Ethernet-based networks, are used for the time data transmission and synchronization in the laboratory with sub-nanosecond precision.

The deduction of the calibration error for the current transformers is split into two parts. For the conventional CT calibrations, the DUT is regarded as an analogue CT. The complex voltage ratio \underline{L}_{XN} of the measuring system, $\underline{L}_{XN} = \underline{U}_X / \underline{U}_N$, is measured by a Digitizer and two calibrated shunts: \underline{Z}_N and \underline{Z}_X . Using the ratio $\underline{E}_{IU,N}$ of the reference current-to-voltage (C-to-V) transformer, $\underline{E}_{IU,N} = \underline{U}_N / \underline{I}_{in} = \underline{U}_N / \underline{I}_{out} \cdot \underline{I}_{out} / \underline{I}_{in} = \underline{Z}_N \cdot \underline{E}_{I,N}$, and the ratio $\underline{E}_{IU,X}$ of the DUT C-to-V transformer, $\underline{E}_{IU,X} = \underline{U}_X / \underline{I}_{in} = \underline{U}_X / \underline{I}_{out} \cdot \underline{I}_{out} / \underline{I}_P = \underline{Z}_X \cdot \underline{E}_{I,X}$, the current ratio $\underline{E}_{I,X}$ of the DUT CT can be calculated as follows:

$$\underline{E}_{I,X} = \underline{L}_{XN} \cdot \underline{E}_{I,N} \cdot \underline{Z}_N / \underline{Z}_X. \quad (1)$$

Besides, the $\underline{E}_{I,X}$ for a CT (DUT) can be defined as

$$\underline{E}_{I,X} = \underline{I}_S / \underline{I}_P = 1 / K_n \cdot (1 + \varepsilon_i) \cdot e^{j \cdot \delta_i} \quad (2)$$

where K_n is the transformer ratio of the rated primary and secondary currents $K_n = I_{P,r} / I_{S,r}$, ε_i and δ_i represent the ratio error and the phase error of the CT. By combining (1) and (2), the errors of the analogue CT are deduced.

For a digital instrument transformer, the ratio $\underline{E}_{I,X}$ can be expressed by $\underline{I}_{mu} / \underline{I}_{in}$ (or equivalently $\underline{U}_{mu} / \underline{U}_{in}$). \underline{I}_{mu} represents the complex fundamental rms current that is calculated from the Discrete Fourier Transform (DFT) of the SVs. \underline{I}_{in} refers to the measured primary current by means of the reference CT $\underline{E}_{I,N}$, the highly accurate shunt \underline{Z}_N and the measured voltage \underline{U}_N of the digitiser. The measured complex primary current is determined according to $\underline{I}_{in} = \underline{U}_N / (\underline{Z}_N \cdot \underline{E}_{I,N})$. In order to relate the two measurements, a sinusoidal signal \underline{U}_{ref} is generated as the phase reference by the waveform generator, programmed without any phase offset ($\arg\{\underline{U}_{ref}\} = 0^\circ$) at channel CH I. This phase reference, which is synchronised to the GPS PPS signal, is connected the Digitiser channel \underline{U}_X ($\underline{U}_X = \underline{U}_{ref}$). The complex voltage ratio \underline{L}_{XN} is measured by a Digitizer $\underline{L}_{XN} = \underline{U}_X / \underline{U}_N = \underline{U}_{ref} / (\underline{I}_{in} \cdot \underline{Z}_N \cdot \underline{E}_{I,N})$. The ratio error ε_i of the digital DUT can be calculated as follows:

$$\varepsilon_i = \underline{I}_{mu} / \underline{I}_{in} - 1 \quad (3)$$

where the rms current I_{in} is determined by $I_{in} = U_N / (Z_N \cdot E_{I,N})$. The phase error δ_i of the digital DUT can be calculated as

$$\delta_i = \arg\{\underline{I}_{mu}\} - \arg\{\underline{I}_{in}\} \quad (4)$$

where the absolute phase of the complex current $\arg\{\underline{I}_{in}\}$ is determined by $\arg\{\underline{I}_{in}\} = \arg\{\underline{U}_{ref}\} - (\arg\{\underline{L}_{XN}\} + \arg\{\underline{Z}_N\} + \arg\{\underline{E}_{I,N}\})$.

III. COMPONENTS OF THE CALIBRATION SYSTEM

The detailed components for the current transformer calibration system, shown in Fig. 1, deal with a programmable two-channel generator for the generation system, a reference current-to-voltage (C-to-V) transformer set as analogue reference CTs and an SV receiver box for the CTs with digital output.

A. Program of the two-channel generator

The LabVIEW program is designed to control and extend the waveform generation of the two-channel generator with three main functions: hardware communication, generation setups and the data stream generation. The flow chart of software is shown in Fig. 2.

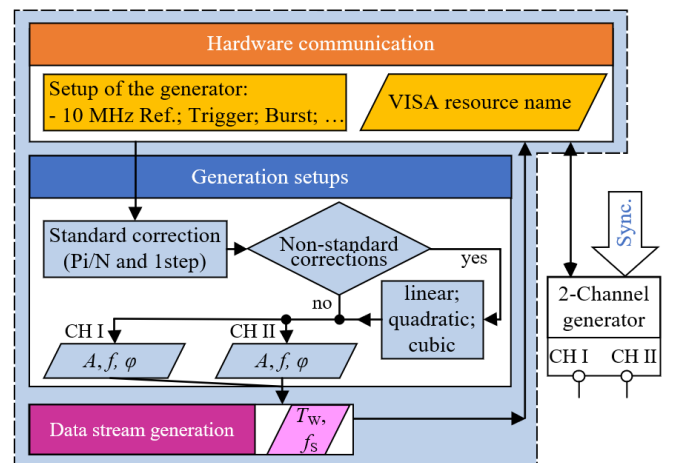


Fig. 2. Flow chart of the Agilent generator LabView-based software platform

The hardware communication (shown as orange blocks) must be correctly set before the signals are sent to the generator. The generation setups (shown as blue blocks) contain the general settings of the signal parameters (A, f, φ), and the phase corrections. Based on the sample rate f_s and the

time duration T_w (shown in the purple block), the arbitrary waveforms are calculated as a data set. Finally, this data set is sent to the generator.

The phase corrections are used for the alignment of the arbitrary waveforms to the reference PPS signal. The phase corrections are differentiated into standard corrections and optionally usable, small non-standard corrections for compensating the generator-internal phase shifts. To avoid the time delay between the reference PPS and the generated signals, a numerical method is designed. The “ideal” mathematical time-quantized voltage waveform is expressed as

$$u_{DAC}(v) = \sqrt{2} \cdot U_{rms} \cdot \sin(B \cdot v + \varphi_0 + \varphi_{step} + x + y) \quad (5)$$

where $0 \leq v \leq T_w \cdot f_s - 1$, $B = 2\pi / N$, $x = \pi / N$ (“Pi/N” phase correction [12], [13]), $\varphi_{step} = 2\pi / N$ (“1-step” phase correction [12], [13]), $N = f_s / f$ (samples per period - SpP) and y refers to the user-defined non-standard phase corrections.

B. The reference C-to-V transformer

The reference C-to-V transformer consists of a current transformer and an associated precise measuring resistor. The rated primary currents of the C-to-V transformer set ranges from 8.3 A to 1500 A. Four commercial zero-flux CTs with rated currents of 50 A (CT50), 200 A (CT200 [8]), 600 A (CT600) and 2 kA (CT1500) were used to establish the reference CTs. To convert the different secondary currents of these CTs into a 1 V output voltage, a resistor box was built, containing six precision resistors from 1 Ω to 20 Ω .

As an example, the symmetrical winding configuration of the added primary of the CT1500 is illustrated in detail in Fig. 3 (a) from a vertical view. The connection scheme for the different primary windings $N_p = 1$ to 4 of the CT1500 is shown in Fig. 3 (b).

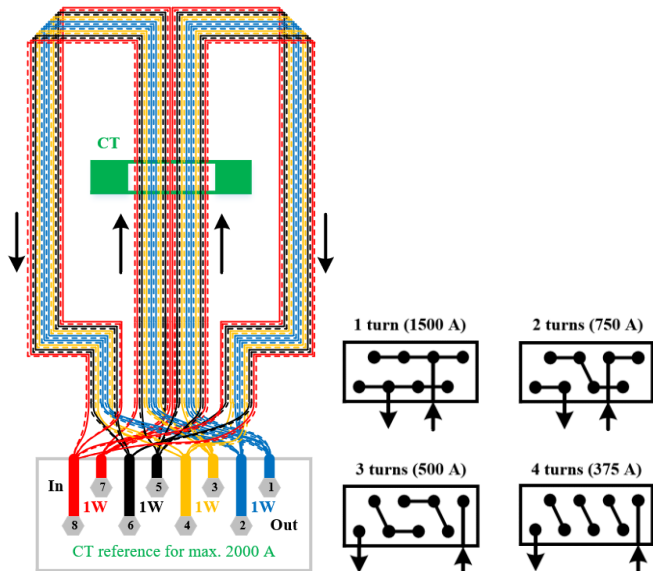


Fig. 3. Configuration design (left) and connection setups (right) of CT1500

The usability and expected metrological characteristics of the window type zero-flux transformer were improved by implementing several symmetrical primary windings to the CT.

The resistor box consists of two power supplies, two separate channels and six precision resistors. The power supply with ± 15 V DC voltage operates the CTs. The

integration of two channels into one box allows a simple and monolithic calibration facilities for the reference CT as against the DUT. The nominal values of the resistors were selected from 1 Ω to 20 Ω . The detailed designs of one measuring resistor are schematically shown in Fig. 4 from various views.

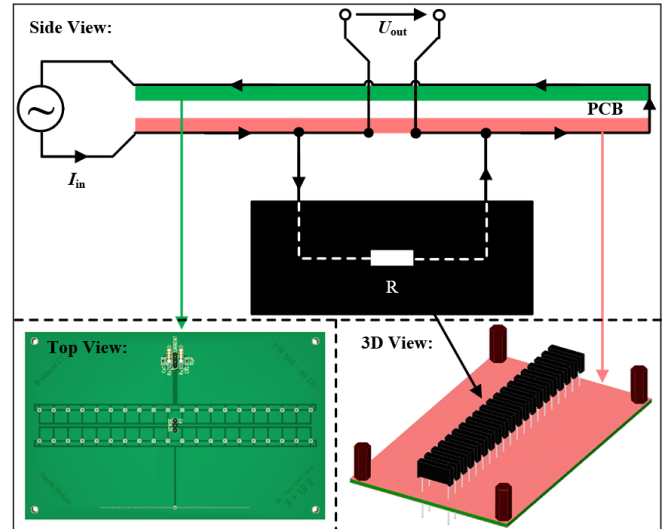


Fig. 4. Designs of the measuring resistor from various views (without a heatsink)

Each measuring resistor R_m is designed to be made up of numbers of resistors R in parallel, an associated printed circuit board (PCB) and a large heatsink. Each single resistor R was selected with a power rating of 1.5 W. The construction of the resistors R in parallel for one R_m value, e.g., twenty 20 Ω resistors in parallel for a 1 Ω measuring resistor, benefits to reduce the power loss inside the resistor. The PCB is designed to minimize the ac errors (ε_m and δ_m) of the measuring resistor by minimizing the effective magnetic field for the resistors. The heatsink is developed later around the resistors.

C. SV receiver box

The self-designed SV receiver is developed to connect SV-based devices with the LabView-based software platform in a computer with integrated analysis of the SV.

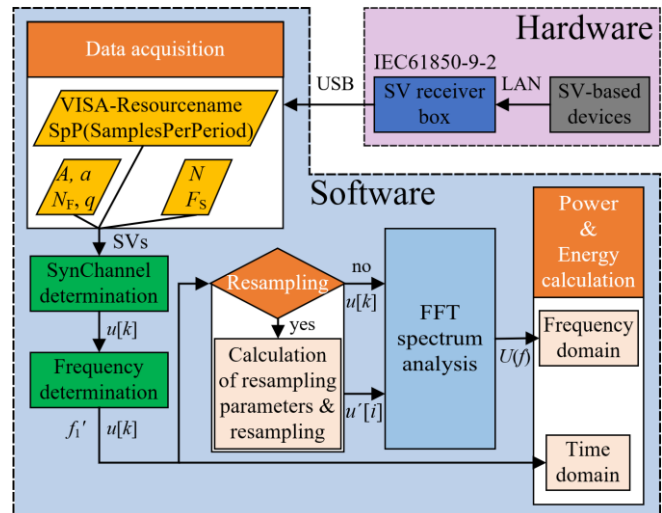


Fig. 5. Flow chart of the SV receiver box LabView-based software platform with hardware connections

To avoid damaging of the sampled values, the SV receiver box offers PC time buffer for a seamless, quasi-real-time digital data processing. In praxis, the SVs, which satisfied

with the standard IEC61869-9, are sent from the SV-based devices, e.g., SAMU/MU, through an Ethernet port. The SV receiver transmits the SVs to the computer through a USB port according to IEC61850-9-2 communication protocol.

The flow chart of the LabView-based software platform, shown in Fig. 5, illustrates the detailed processes according to different function modules. Firstly, the VISA-ResourceName and parameters (SpP; A , a , N_F and q : the resampling parameters; N , F_s : the sampling parameters) are required for the data acquisition. After the transfer of the data (SVs), the channel for the synchronisation (SynChannel) is selected and the frequency of the signal is determined. The resampling processing [14] can be chosen when the detected signal frequency is not synchronised to the given sampling parameters. The FFT spectrum analysis is supposed to determine rms values and phase angles of the voltages and currents of the SV in the frequency domain. Based on these values, the required current I_{mu} and its phase $\arg\{I_{mu}\}$ can be extracted for calculating the current error and phase displacement - see (3) and (4) - of the SV-based device.

IV. VALIDATIONS OF THE CALIBRATION SYSTEM

The validations of the CT calibration system, corresponding to the described components in Section III, are divided into three parts: results of the programmable two-channel generator, characterisation of the reference C-to-V transformer set and validations of the SVs.

A. Calibration results of the programmable two-channel generator

The calibrations with the standard phase corrections (Pi / N & 1 step phase corrections) for the programmable two-channel generator were divided into two aspects: the characterization of the absolute phase shift between the generated signals of the generator and the GPS PPS time reference and the characterization of the relative phase shift between the two generated signals of the two channels. The absolute phase error $\Delta\varphi_{abs}$ was determined from the time difference Δt_{abs} between the zero gear of the generated phase reference signal t_{CHI} and the positive edge of the PPS clock t_{PPS} . An oscilloscope has been used for determining this time difference $\Delta t_{abs} = t_{CHI} - t_{PPS}$. The relative phase error $\Delta\varphi_{rel}$ between the two channels was measured by the precision 2-channel measuring system [15].

The investigated parameters for the calibration measurements are classified into two groups for each characterization aspect: the generation parameters of the SV data stream (f_s , i.e., the SpS and T_W) and the general settings of the signal parameters (f_0 , A_0 , φ_0 and f_h , A_h , φ_h for a dual-tone signal with the h^{th} overtone as well as f , A , φ for a sinusoidal or square signal).

a) *Absolute phase errors* $\Delta\varphi_{abs}$: For example, a measurement result for deriving the absolute phase errors $\Delta\varphi_{abs}$ is shown in Fig. 6, which contains many modified details from the oscilloscope screen shot. The used parameter values were regarded as default values for the general measurement. Besides, since the resolution of the oscilloscope is in nano-second range, the oscilloscope measurement almost overlaps the generated signals from the two-channel generator.

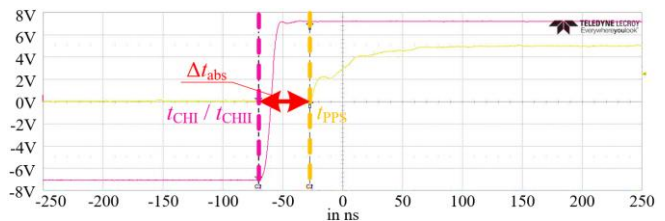


Fig. 6. The time difference between the zero gear of the generated signal (the pink curve) and the positive edge of the PPS clock (the yellow curve) in the oscilloscope. (square wave - general settings: $f = 50$ Hz, $U = 5$ V; the generation parameters: $f_s = 100$ kHz, $T_W = 1$ s; with Pi / N & 1 step phase corrections)

For the measurement shown in Fig. 6, the time difference Δt_{abs} (marked as red in Fig. 6) is obtained by the generated signal of one channel (shown as a pink curve) and the reference PPS clock (shown as a yellow curve). To avoid the reading error due to the reflection of the electric signals in the coaxial cable, the times t_{CHI} / t_{CHII} and t_{PPS} were all directly determined at the beginning of the rising edge of the square wave signals or at the beginning of the positive edge of the sinusoidal signals. Finally, the absolute phase errors were calculated as $\Delta\varphi_{abs} = 2\pi f \cdot \Delta t_{abs}$.

Preliminary investigations on the absolute phase errors $\Delta\varphi_{abs}$ of the generated signals from the two-channel generator showed that the amplitude linearity (A_0), the phase linearity (φ_0) of the generated signals and the time window for the SV generation of the generator ($T_W = 1$ s or 10 s) had no significant influence on $\Delta\varphi_{abs}$. Moreover, the absolute phase errors of a sinusoidal signal had almost the same errors as its corresponding dual-tone signals ($A_h = 10\%A_0$, h up to 51). By varying fundamental frequency of the signals at 50 Hz, 60 Hz and 100 Hz, the absolute phase errors ($\Delta\varphi_{abs,50Hz} = -7.7$ μ rad, $\Delta\varphi_{abs,60Hz} = -10.6$ μ rad, $\Delta\varphi_{abs,100Hz} = -15.6$ μ rad) had small a difference of below 10 μ rad with SpS = 100,000.

In order to have a better recognition of the results from the oscilloscope's display, the square wave signals were generated for the measurements of SV generation with various SpS. To avoid the surrounding disturbance of the signals at power frequency, the signal frequency was set as 52 Hz. Moreover, different measurement setup, e.g., various cable length for the connections, leads to a small drift for the absolute phase errors in μ rad range. The results regarding the different SpS ranging from 5,000 to 500,000 with a certain measurement setup are shown in TABLE I.

TABLE I. ABSOLUTE PHASE ERRORS OF THE GENERATED SIGNALS FROM THE TWO-CHANNEL GENERATOR REGARDING THE SpP WITH Pi / N & 1 STEP PHASE CORRECTIONS

SpS	SpP	$\Delta t_{abs}(\text{CH I - PPS})$ in μ s	$\Delta\varphi_{abs}(\text{CH I - PPS})$ in μ rad	$\Delta t_{abs}(\text{CH II - PPS})$ in μ s	$\Delta\varphi_{abs}(\text{CH II - PPS})$ in μ rad
5000	96.2	-5.65	-1845.88	-5.65	-1846.54
10000	192.3	-2.70	-883.56	-2.71	-884.05
25000	480.8	-0.94	-306.21	-0.94	-306.26
50000	961.5	-0.35	-114.21	-0.35	-113.99
75000	1442.3	-0.16	-51.15	-0.16	-50.84
100000	1923.1	-0.06	-18.93	-0.06	-18.70
116000	2230.8	0.00	-1.01	-0.02	-4.95
150000	2884.6	0.06	18.41	0.04	14.38
250000	4807.7	0.12	38.50	0.12	38.99
500000	9615.4	0.12	38.40	0.12	38.77

The generated signals are square wave signals with parameters of $U = 5$ V, $f_0 = 52$ Hz

The results from TABLE I demonstrate that the absolute phase errors of the two channels of the generator were almost

identical with each other for a certain SpS. With increasing of the SpS, the absolute phase errors changed from around -1846 μrad with SpS = 5,000 to around +38 μrad with SpS = 500,000. After several attempts, the absolute phase errors approached to zero with SpS = 116,000. For the calibrations of a CT with a digital output, the absolute phase errors in TABLE I can be used directly as the phase corrections to the PPS signal, $\arg\{\underline{U}_{\text{PPS}}\}$, for the reference phase, $\arg\{\underline{U}_{\text{ref}}\}$, in (4).

b) *Relative phase errors $\Delta\phi_{\text{rel}}$* : The calibration measurements were executed by five aspects: the amplitude linearity (from 2% $\cdot A_0$ to 100% $\cdot A_0$) of the investigated signal, the phase linearity (ϕ_0 from 0 degree to 180 degree) of the investigated signal, various generator clock rate (f_s from 10 kHz to 500 kHz) for the SV generation of the generator, various time window (T_W from 1 s to 10 s) for the SV generation of the generator and the influence by a dual-tone signal with an odd harmonics (up the 49th order). One generated signal of the generator was set as an invariant reference signal ($A_0 = 5 \text{ V}$, $f_0 = 52 \text{ Hz}$), which was connected to the reference channel of the measuring system. The parameters: f_s (default: $f_s = 100 \text{ kHz}$), T_W (default: $T_W = 1 \text{ s}$) and the option for Pi/N & 1 step phase corrections were programmed to be varied contemporaneously for both channels of the generator. As a result, the relative phase errors between the generated signals from two-channel generator stay below 10 μrad for the complete investigations.

B. Characterisation of the reference C-to-V transformer

The final accomplished set of reference current transformers and the associated precise measuring resistor box are presented in Fig. 7. The reference CTs, shown in Fig. 7 (above) from link to right, are respectively the CT50, CT200, CT1500 and CT600. The front panel of the associated precise measuring resistor box is presented in Fig. 7 (below).



Fig. 7. Photo of the accomplished wideband current-to-voltage transformer set for currents up to 2 kA. The symmetrical current transformers (above) and the front panel of the associated precise measuring resistor box (below)

According to the previous work [8], the characterisation of the C-to-V transformers was carried out by separating the behaviour at power frequency and the frequency response. The errors of the current transformers ($\varepsilon_i(f)$ and $\delta_i(f)$) are represented by $\varepsilon_i(f) = \varepsilon_i(f_0) + \Delta\varepsilon_i(f)$ and $\delta_i(f) = \delta_i(f_0) + \Delta\delta_i(f)$, where $\varepsilon_i(f_0)$ and $\delta_i(f_0)$ refer to the CT errors at power frequency and $\Delta\varepsilon_i(f)$ and $\Delta\delta_i(f)$ refer to the frequency response of the CTs. A step-up calibration was especially used when the frequency response of the CTs is determined. So far, the calibration measurements at power frequency of the reference current transformer set have been completed. The errors of the

reference current transformer set were within $\pm 10 \mu\text{A/A}$ and μrad at 50 Hz. In addition, the initial frequency response measurements of the first two CTs (CT50 and CT200) showed that the ac errors at a frequency of 12 kHz were below 0.1 % and 0.2 crad with the expanded uncertainties are below 0.01 % and 0.03 crad ($k = 2$).

Furthermore, the errors of the self-developed measuring resistors are represented by a ratio error ε_R and a time constant τ_Z , where ε_R was obtained by the calibration at power frequency and τ_Z was derived from the phase behaviour of the frequency response measurements. As a consequence, the calibrated results of the 6 measuring resistors are listed in TABLE II.

TABLE II. ERRORS OF MEASURING RESISTORS. RATIO ERRORS OF RESISTORS AT POWER FREQUENCY WITH 100% RATED INPUT CURRENT AND PHASE ERRORS OF RESISTORS FOR FREQUENCIES FROM 16 HZ TO 12 KHZ WITH 80% RATED INPUT CURRENT

R_m	I_{nom}	ε_R in $\mu\Omega/\Omega$	U_{eR} in $\mu\Omega/\Omega$ ($k = 2$)	τ_Z in ns	$U(\tau_Z)$ in ns ($k = 2$)
1 Ω	1 A	-1.2	2.5	0.2	4
2.5 $\Omega - R_a$	400 mA	0.7	2.4	0.0	3
2.5 $\Omega - R_b$	400 mA	0.3	2.4	0.0	3
5 Ω	200 mA	0.6	2.5	0.0	3
10 Ω	100 mA	-1.6	1.7	-0.3	3
20 Ω	50 mA	-2.0	2.5	-1.1	3

The ratio errors of the 6 measuring resistors were below $\pm 2 \mu\Omega/\Omega$ at power frequency with expanded uncertainties below $\pm 3 \cdot 10^{-6}$ ($k = 2$). The time constant was about below $\pm 1 \text{ ns}$ with the attained expanded uncertainties below $\pm 4 \text{ ns}$.

C. Validation of the SVs

To validate the accuracy of the received SVs from the SV receiver box, the plausibility of the generated SVs needs to be validated in the first place. Therefore, the validation measurements the SVs are assigned into two parts: the validation of the SV generation and the validation of the SV receiving.

For laboratory validation of the SV generation, a microcontroller-based SV generator box and the corresponding LabView-based program were developed for sending the SV-data over the ethernet using the IEC91850-9-2 communication protocol. The basic module box is a 32-bit ARM Cortex-M4 CPU with an ethernet and a USB port. Three-phase four-wire (L_1, L_2, L_3, L_N) currents and voltages with 1 mA current resolution and 10 mV voltage resolution are programmed as the SV data stream through the USB port. A one-period signal is initially programmed to the SV generator box and repetitively sent to the SV-based devices. The beginning of an SV data set is signaled by a rising edge on the PPS output. The sample rates for the SV generation were configured as 4000 Hz (Application Service Data Unit: ASDU = 1), 4800 Hz (ASDU = 1 or ASDU = 2), 5760 Hz (ASDU = 1) and 14400 Hz (ASDU = 6). In addition, the SV generator box was considered as a substitute for the devices with the digital output (e.g., a SAMU) and can be used for the validation of an SV-based measuring device (e.g., for digital energy meters) without any numerical loss.

The validation of the SV generation mainly deals with the round-off function in LabVIEW program. The errors were determined by the currents and voltages difference between the SVs directly generated by LabVIEW and the SVs sent to the SV-based devices. The results of the SV generation for L_1

are presented in Fig. 8 for instance. Dual-tone signals ($f_0 = 50$ Hz, $I_0 = 1$ kA, $\varphi_{0_I} = 0^\circ$, $U_0 = 100$ kV, $\varphi_{0_U} = 0^\circ$) with the 3rd harmonics (10 % amplitude, zero phase offset) were generated for the three-phase currents and voltages.

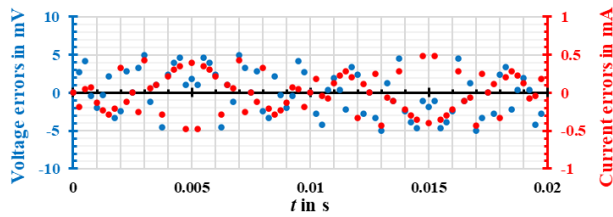


Fig. 8. The errors of generated voltages and currents (L_1) in SV generator program

As shown in Fig. 8, the voltage errors stay within ± 5 mV and the current errors stay within ± 0.5 mA, as anticipated due to the 1 mA current resolution and 10 mV voltage resolution of the standardised data stream [1], [2]. It can therefore be concluded that the sampled values, sent by the SV generator box, are plausible and numerically accurate within their resolutions.

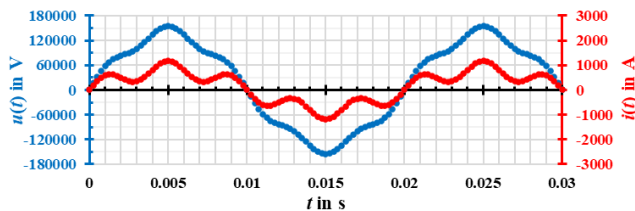


Fig. 9. The received voltages and currents (L_1) of SV receiver box in time domain

Corresponding to the SV generation for Fig. 8, the received SVs of L_1 from the SV receiver box are shown in Fig. 9. The diagram shows that the SV receiver box received the repeated one-period signal ($t > 0.02$ s) from the SV generator box. Moreover, the differences between the sent and received SVs equalled to zero. This means that the SV receiver box receives exactly what is sent to it. Eventually, similar results were obtained by L_2 , L_3 and L_N as well.

V. CONCLUSION

In conclusion, the proposed calibration system has been applied for calibrating at least three different types of analogue current sensors (conventional inductive CTs, electronic CTs and Rogowski coils) and two SAMUs from different companies, as planned in FutureGrid II. The absolute phase errors of the two-channel generator to the GPS PPS time reference are mainly depended on the SpS and can be configured to almost zero. The errors of the reference current transformer set are within $\pm 10 \mu\text{A/A}$ and μrad at power frequency. According to IEC 61869-13 [5] for a SAMU and IEC 61869-6 [16] for a low-power instrument transformer (LPIT), the anti-aliasing filter attenuation for the half of the sampling rates (up to 14.4 kHz) up to 7.2 kHz shall be greater and equal to 40 dB. The uncertainties caused by the two-channel generator, the set of reference current transformers and the precision 2-channel measuring system are well below 10^{-3} up to 12 kHz. Compared to the limits by the internal anti-aliasing filter of the DUT, the uncertainties of the proposed measuring system strictly meet the requirements. The SV receiver box is firstly validated for all sample rates with 1 ASDU. Additionally, preliminary calibrations of a SAMU are currently being executed.

Further complete calibrations of the integrated C-to-V transformer set and the SAMU as well as the corresponding measurement uncertainties will be accomplished in the prospective work. The SV receiver box will be extended for further sample rates with 2 ASDUs and 6 ASDUs according to [1]. Moreover, small phase errors of the phase reference signal of the generator can be software-compensated with a non-standard phase correction.

ACKNOWLEDGMENT

This project has received funding from the EMPIR programme co-financed by the Participating States and from the European Union's Horizon 2020 research and innovation programme.

REFERENCES

- [1] *Instrument Transformers - Part 9: Digital interface for instrument transformers*, IEC 61869-9, 2016.
- [2] *Communication networks and systems for power utility automation - Part 9-2: Specific communication service mapping (SCSM) - Sampled values over ISO/IEC 8802-3*, IEC 61850-9-2, 2005.
- [3] (2017) The Future Grid II website [Online]. Available: <https://www.vtt.fi/sites/FutureGrid2/> [May 2021].
- [4] T. A. Lehtonen, "Harmonic Power Standard of VTT MIKES," in *IEEE Transactions on Instrumentation and Measurement*, vol. 68, no. 6, pp. 2047-2052, June 2019, doi: 10.1109/TIM.2018.2880056.
- [5] *Instrument Transformers - Part 13: Stand-alone merging unit (SAMU)*, IEC 61869-13, 2019.
- [6] B. Djokic and H. Parks, "A Synchronized Current-Comparator-Based Power Bridge for Calibrating Analog Merging Units," *2018 Conference on Precision Electromagnetic Measurements (CPEM 2018)*, 2018, pp. 1-2, doi: 10.1109/CPEM.2018.8501127.
- [7] B. Djokic and H. Parks, "Calibration of Electricity Meters with Digital Input," *2018 Conference on Precision Electromagnetic Measurements (CPEM 2018)*, 2018, pp. 1-2, doi: 10.1109/CPEM.2018.8500803.
- [8] Chen Y., Mohns E., Badura H., Raether P., "Development of a Wideband Current-to-Voltage Transformer Set for Currents up to 2 kA", *2020 Conference on precision Electromagnetic measurements (CPEM)*, 24-28 August 2020; doi: 10.1109/CPEM49742.2020.9191814.
- [9] E. Mohns, J. Meisner, G. Roeissle, M. Seckelmann and M. Korejwo: "A Wideband Current Transformer Bridge," *4rd IEEE International Workshop on Applied Measurements for Power Systems, AMPS 2013*, September 2013, Aachen, Germany.
- [10] T.Möhring, E.Mohns, M.Schmidt, T.Funck: "Characterization of a 2-Channel Digitizer with Differential Inputs," *CPEM 2012 Digest*, Washington, July 2012.
- [11] White Rabbit LEM [Online]. Available: <https://sevensols.com/home/timing-products/wr-lem/> [May 2021].
- [12] E. Mohns, A. Mortara, H. Cayci, E. Houtzager, S. Fricke, M. Agustoni, B. Ayhan: "Calibration of Commercial Test Sets for Non-Conventional Instrument Transformers," *IEEE International Workshop on Applied Measurements for Power Systems, AMPS 2017*, September 2017, Liverpool, UK, DOI: 10.1109/AMPS.2017.8078324.
- [13] H.-D. Schlemper, D. Fuchsle, G. Ramm, J. Widmer: "Test and Application of Non-Conventional Multi-Purpose Voltage and Current Transducers", *CIGRE, Session 2004*, A3-108.
- [14] Y. Chen, E. Mohns, M. Seckelmann and d.R. Soeren, "Precise Amplitude and Phase Determination Using Resampling Algorithms for Calibrating Sampled Value Instruments," *Sensors*. 2020; 20(24):7345. pp. 1-21, doi: <https://doi.org/10.3390/s20247345>.
- [15] E. Mohns, J. Chunyang, H. Badura and P. Raether: "A Fundamental Step-Up Method for Standard Voltage Transformers Based on an Active Capacitive High-Voltage Divider," *IEEE Trans. Instrum. Meas.*, vol. 68, no. 6, pp. 2121-2128, June 2019, DOI: 10.1109/TIM.2018.2880055.
- [16] *Instrument Transformers - Part 6: Additional general requirements for low-power instrument transformers*, IEC 61869-6, 2016.